

Aircraft Conflict Detection and Resolution using Mixed Geometric and Collision Cone Approaches

Jennifer Goss¹, Rahul Rajvanshi² and Kamesh Subbarao³
University of Texas at Arlington, Arlington, TX 76019-0018

This paper considers the problem of avoidance of conflict or collision between two aircraft in a 3-D environment utilizing current positions and velocities using a mixed geometric and collision cone approach. Analytical results are obtained for certain special cases and numerical optimization techniques are used to search for solutions to the most general cases. The results are optimal as they tend to minimize the velocity vector changes and thus result in minimum deviations from nominal trajectory so as to avoid conflict. It is assumed that the aircraft is able to change its velocity, heading and elevation angles independently and all combinations of these three degrees of freedom are investigated for obtaining the resolution strategies. The simulation results also include explicit bounds on the airspeeds (lower and upper limits) and turning rates to enforce realistic scenarios.

I. Introduction

THE aircraft conflict detection and resolution has been the object of intensive research, over the past several years following the sustained growth of past and forecasted air traffic. A comprehensive survey of conflict detection and resolution methods is presented in Ref. [1]. This problem of collision avoidance is a fundamental requirement in the path to automating air traffic controllers in cluttered civilian air space. This and a close cousin of this problem in the motion planning of mobile robots have been extensively studied in Refs. [4], [5], [6], [7] and [8]. The aircraft collision avoidance problem differs from most classes of obstacle avoidance problems studied in the robotics literature due to the fact that the obstacles are never stationary. In addition, air speed restrictions and turning rate restrictions on an aircraft severely limit the maneuvering zone thereby reducing the solution space. The planar engagement of two aircrafts was studied analytically in Ref. [2], which is referred to as the geometric optimization approach. Ref. [3] presents a novel collision cone approach to tackle the obstacle avoidance problem in a dynamic environment utilizing results from missile guidance strategies. The results reported therein as in Ref. [2] were restricted to the planar engagement as the problem being dealt with was that of obstacle avoidance in robotic vehicles.

Among a number of optimization methods that are used for solving conflict resolution problems, [1] states that generally for optimized conflict resolution either a set of predefined rules or an Optimal Control Theory (OCT) using a cost function can be used. Genetic Algorithms and approaches based on Force field models, wherein each aircraft is modeled as a charged particle and electrostatic equations are used to calculate repulsive forces between them to determine resolution maneuvers could be employed. In [2] the author validates the analytical results obtained with numerically generated results of the Semi-Definite Programming (SDP) method that uses a formal optimization process to minimize a performance index. References [4, 5, 6, 7, 8] mainly refer to Robot motion planning and use techniques like potential fields to design an optimal path. Visibility graphs and cell decomposition methods are other optimization techniques that have also been used to address this problem.

In this paper this problem is particularized to a 3-D environment by extending the analytical results presented in both Ref. [2] and [3]. Conflict detection and resolution is addressed in a 3-D environment using information of current positions and instantaneous velocity vectors. A zero wind field is assumed and the solution methodology hinges upon construction of general collisions scenarios geometrically so as to calculate a minimum distance metric (D_{\min}) between two non-parallel vectors.

¹ Graduate Student, Department of Mechanical and Aerospace Engineering

² Graduate Student, Department of Mechanical and Aerospace Engineering

³ Assistant Professor, Member AIAA, Department of Mechanical and Aerospace Engineering, Phone: 817 272 7467, Email: subbarao@mae.uta.edu

The rest of the paper is organized as follows: The problem of conflict detection is introduced along with the geometric constructions, followed by derivation of analytical expressions for conflict resolution and finally some sample simulations are presented to highlight the efficacy of the detection and resolution strategies.

II. Conflict Detection

Let $\mathbf{P}_A(x_A, y_A, z_A)$ and $\mathbf{P}_B(x_B, y_B, z_B)$ represent the position coordinates of Aircraft A and B respectively relative to an Earth-fixed axes system as shown in Figure 1; χ_{PA} and χ_{PB} are the corresponding heading angles of the position vectors measured from the X-axis; σ_{PA} and σ_{PB} are the corresponding elevation angles which the position vectors of the aircrafts make with the XY plane. Let \mathbf{R}_{LOS} represent the line-of-sight (LOS) vector from Aircraft A to Aircraft B; the magnitude of this vector is R_{LOS} , and χ_{LOS} and σ_{LOS} are its heading and declination angles.

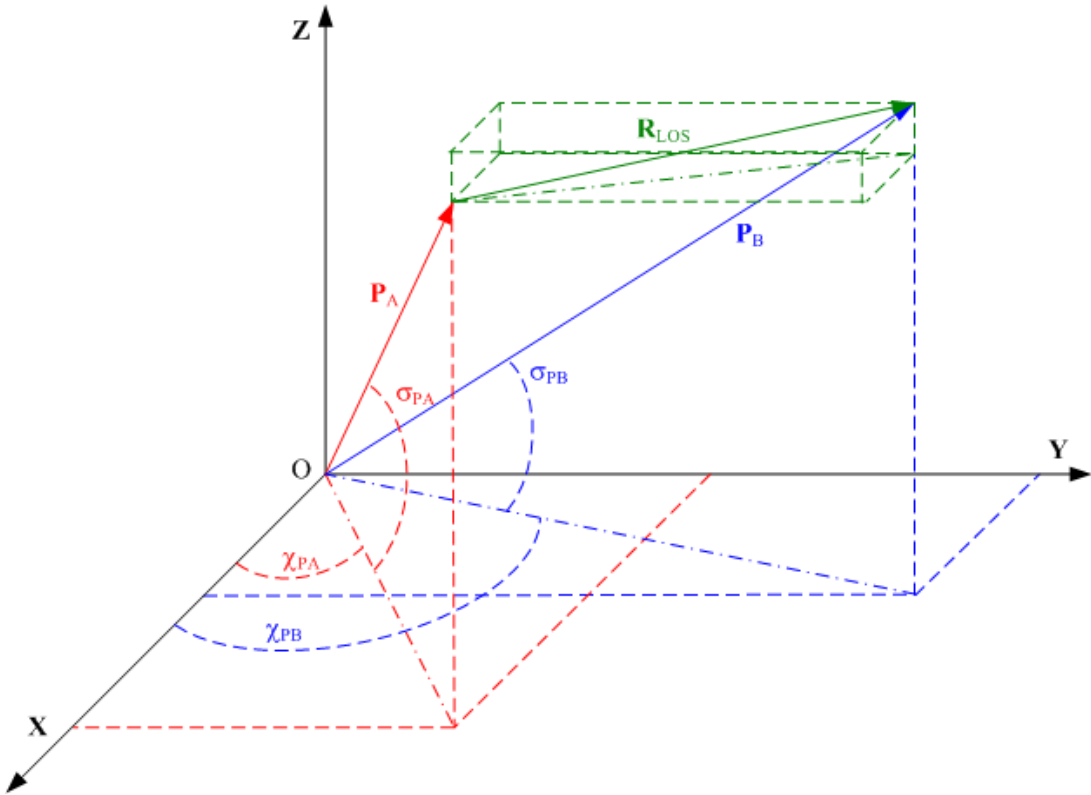


Figure 1: Position vectors of Aircraft A and B and Line-of-Sight Vector, \mathbf{R}_{LOS} .

A. Line of Sight (LOS) construction

Let R_X, R_Y, R_Z be the components of \mathbf{R}_{LOS} . Correspondingly the components of \mathbf{P}_A are represented as P_{AX}, P_{AY}, P_{AZ} and those of \mathbf{P}_B are represented by P_{BX}, P_{BY}, P_{BZ} . The components of the LOS can computed as,

$$R_X = P_{BX} - P_{AX} \quad (1)$$

Where $P_{BX} = P_B \cos \sigma_{PB} \cos \chi_{PB}$ and $P_{AX} = P_A \cos \sigma_{PA} \cos \chi_{PA}$, the magnitude of the position vectors of Aircraft A and Aircraft B are

$$P_A = \sqrt{x_A^2 + y_A^2 + z_A^2} \text{ and } P_B = \sqrt{x_B^2 + y_B^2 + z_B^2} \text{ respectively.} \\ \therefore R_X = P_B \cos \sigma_{PB} \cos \chi_{PB} - P_A \cos \sigma_{PA} \cos \chi_{PA} \quad (2)$$

Similarly, $R_Y = P_{BY} - P_{AY}$ where $P_{BY} = P_B \cos \sigma_{PB} \sin \chi_{PB}$ and $P_{AY} = P_A \cos \sigma_{PA} \sin \chi_{PA}$

$$\therefore R_Y = P_B \cos \sigma_{PB} \sin \chi_{PB} - P_A \cos \sigma_{PA} \sin \chi_{PA} \quad (3)$$

And $R_Z = P_{BZ} - P_{AZ}$ where $P_{BZ} = P_B \sin \chi_{PB}$ and $P_{AZ} = P_A \sin \chi_{PA}$

$$\therefore R_Z = P_B \sin \chi_{PB} - P_A \sin \chi_{PA} \quad (4)$$

The Line-of-sight vector is: $\mathbf{R}_{LOS} = R_X \hat{x} + R_Y \hat{y} + R_Z \hat{z}$

The magnitude, heading and declination angles of the LOS are given as $R_{LOS} = \sqrt{R_X^2 + R_Y^2 + R_Z^2}$ or

$$R_{LOS} = \sqrt{(x_B - x_A)^2 + (y_B - y_A)^2 + (z_B - z_A)^2} \quad (5)$$

$$\chi_{LOS} = \tan^{-1} \left(\frac{R_Y}{R_X} \right) = \chi_R \quad (6)$$

$$\sigma_{LOS} = \tan^{-1} \left(\frac{R_Z}{\sqrt{R_X^2 + R_Y^2}} \right) = \sigma_R \quad (7)$$

The collision scenario is then studied using this line-of-sight vector and its “behavior” with respect to the relative velocity between the two aircraft in the 3-D environment (\mathbf{V}_{rel}).

B. Relative Velocity Construction

Let $\mathbf{V}_A (V_{AX}, V_{AY}, V_{AZ})$ and $\mathbf{V}_B (V_{BX}, V_{BY}, V_{BZ})$ represent the velocities of aircraft A and B respectively relative to the same earth fixed axes system described earlier. Figure 2 shows \mathbf{V}_A and \mathbf{V}_B with the origin translated to Aircraft A's position, V_A and V_B are the corresponding speeds; χ_A and χ_B are the corresponding heading angles of the velocity vectors measured from the X-axis; σ_A and σ_B are the corresponding elevation angles which the velocity vectors of the aircrafts make with the XY plane. Let \mathbf{V}_{rel} represent the relative velocity vector of Aircraft B with respect to A; the magnitude of this vector is V_{rel} , and χ_{rel} and σ_{rel} are its heading and elevation angles respectively.

The velocity of Aircraft A, \mathbf{V}_A can be expressed as

$$\mathbf{V}_A = V_{AX} \hat{x} + V_{AY} \hat{y} + V_{AZ} \hat{z} \quad (8)$$

The x, y and z components of the velocity vector of Aircraft A are trivially computed as

$$\begin{aligned} V_{AX} &= V_A \cos \sigma_A \cos \chi_A, V_{AY} = V_A \cos \sigma_A \sin \chi_A \text{ and } V_{AZ} = V_A \sin \sigma_A \\ \therefore \mathbf{V}_A &= V_A \cos \sigma_A \cos \chi_A \hat{x} + V_A \cos \sigma_A \sin \chi_A \hat{y} + V_A \sin \sigma_A \hat{z} \end{aligned} \quad (9)$$

Similarly the velocity of Aircraft B, \mathbf{V}_B can be expressed as

$$\mathbf{V}_B = V_{BX} \hat{x} + V_{BY} \hat{y} + V_{BZ} \hat{z}$$

The x, y and z components of the velocity vector of Aircraft B are computed as

$$\begin{aligned} V_{BX} &= V_B \cos \sigma_B \cos \chi_B, V_{BY} = V_B \cos \sigma_B \sin \chi_B \text{ and } V_{BZ} = V_B \sin \sigma_B \\ \therefore \mathbf{V}_B &= V_B \cos \sigma_B \cos \chi_B \hat{x} + V_B \cos \sigma_B \sin \chi_B \hat{y} + V_B \sin \sigma_B \hat{z} \end{aligned} \quad (10)$$

The cosine of the angle between the two aircraft velocity vectors \mathbf{V}_A and \mathbf{V}_B is given as

$$\cos(\angle \mathbf{V}_A, \mathbf{V}_B) = \frac{\mathbf{V}_A \cdot \mathbf{V}_B}{V_A V_B}. \text{ Thus from the dot product between the two velocity vectors i.e.,}$$

$$\mathbf{V}_A \cdot \mathbf{V}_B = V_A V_B (\cos \sigma_A \cos \chi_A \cos \sigma_B \cos \chi_B + \cos \sigma_A \sin \chi_A \cos \sigma_B \sin \chi_B + \sin \sigma_A \sin \sigma_B)$$

$$\mathbf{V}_A \cdot \mathbf{V}_B = V_A V_B (\cos \sigma_A \cos \sigma_B \cos(\chi_A - \chi_B) + \sin \sigma_A \sin \sigma_B)$$

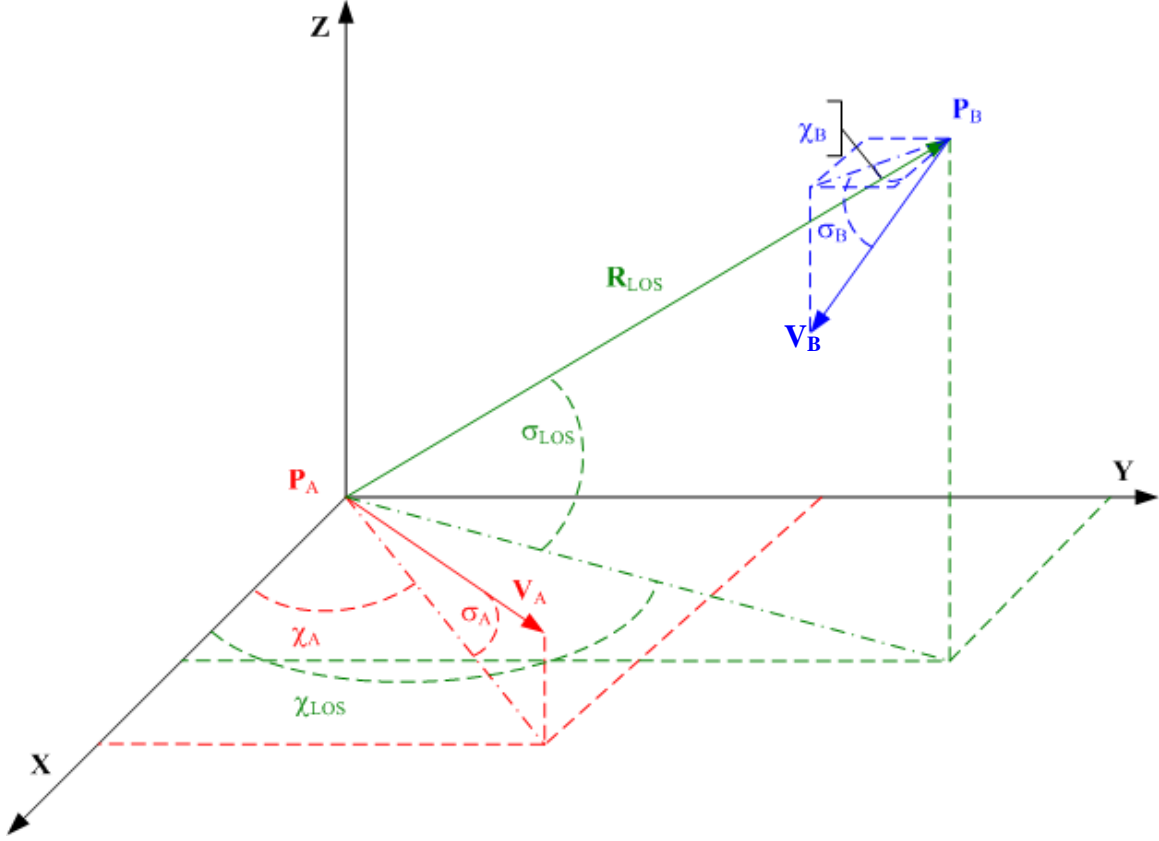


Figure 2: Velocity Vectors of Aircraft A and B

We obtain the cosine of angle between the two velocity vectors as

$$\therefore \cos(\angle \mathbf{V}_A, \mathbf{V}_B) = (\cos \sigma_A \cos \sigma_B \cos(\chi_A - \chi_B) + \sin \sigma_A \sin \sigma_B) \quad (11)$$

The relative velocity vector of Aircraft B with respect to Aircraft A is not known in terms of the available information as, $\mathbf{V}_{rel} = (\mathbf{V}_B - \mathbf{V}_A)$

$$\text{The magnitude of the relative velocity is } V_{rel} = \sqrt{V_A^2 + V_B^2 + 2V_A V_B \cos(\angle \mathbf{V}_A, \mathbf{V}_B)} \quad (12)$$

with the heading angle given by,

$$\chi_{rel} = \tan^{-1} \left(\frac{V_{relY}}{V_{relX}} \right) = \tan^{-1} \left(\frac{V_B \cos \sigma_B \sin \chi_B - V_A \cos \sigma_A \sin \chi_A}{V_B \cos \sigma_B \cos \chi_B - V_A \cos \sigma_A \cos \chi_A} \right) \quad (13)$$

and the elevation angle given by

$$\sigma_{rel} = \tan^{-1} \left(\frac{V_{relZ}}{\sqrt{V_{relX}^2 + V_{relY}^2}} \right) \quad (14)$$

The individual components are then calculated as follows,

$$\begin{aligned} V_{relX}^2 &= (V_B \cos \sigma_B \cos \chi_B - V_A \cos \sigma_A \cos \chi_A)^2 \\ V_{relY}^2 &= (V_B \cos \sigma_B \sin \chi_B - V_A \cos \sigma_A \sin \chi_A)^2 \\ V_{relZ}^2 &= (V_B \sin \sigma_B - V_A \sin \sigma_A)^2 \end{aligned} \quad (15)$$

Rewriting Eq. (5), (6) and (7) we have

$$R_{LOS} = \sqrt{(x_B - x_A)^2 + (y_B - y_A)^2 + (z_B - z_A)^2}$$

$$\chi_{LOS} = \tan^{-1}\left(\frac{R_Y}{R_X}\right)$$

$$\sigma_{LOS} = \tan^{-1}\left(\frac{R_Z}{\sqrt{R_X^2 + R_Y^2}}\right)$$

Eqs. (5), (6), (7) and (12), (13), (14) form the basis of the geometric optimization approach to aircraft conflict detection and resolution. It should be noted that the “ATAN2” function should be used in order to compute the values of angles in the correct quadrant.

C. Conflict Zone Construction

From the geometry of the LOS and the Relative velocity vectors as shown in Figure 3, we see that the two aircraft will encounter a minimum separation distance, d_{\min} , at some point in the future and this d_{\min} vector is calculated

as follows, $\mathbf{d}_{\min} = \mathbf{R}_{LOS} - \frac{\mathbf{R}_{LOS} \cdot \mathbf{V}_{rel}}{\|\mathbf{V}_{rel}\|^2} * \mathbf{V}_{rel}$

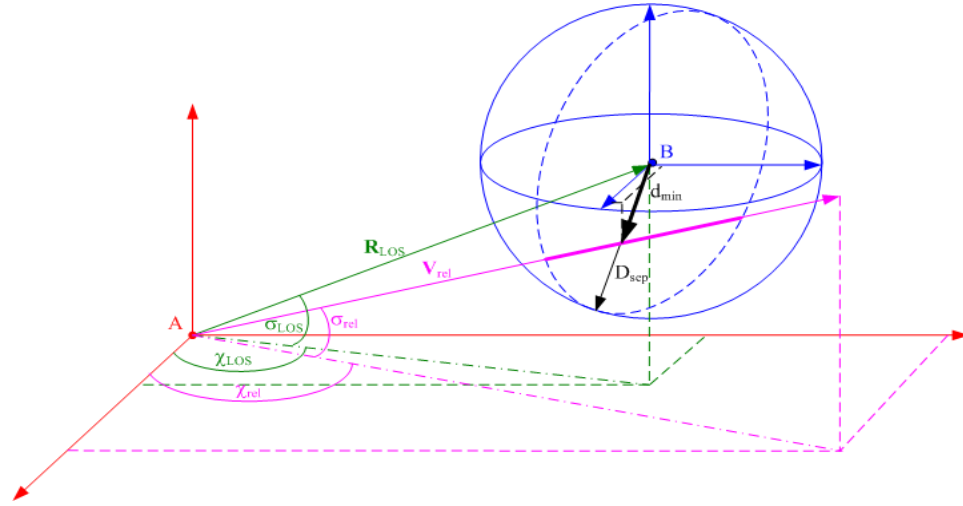


Figure 3: Aircraft Line-of-Sight and relative velocity vectors and minimum separation, d_{\min}

Further, the horizontal component of \mathbf{d}_{\min} is computed as

$$d_{\min}^H = R_{LOS} \text{ If } |\chi_{rel} - \chi_{LOS}| \geq 90^\circ; \text{ ELSE}$$

$$d_{\min}^H = R_{LOS} \cos(\sigma_{rel} - \sigma_{LOS}) \sin(\chi_{rel} - \chi_{LOS}) \quad (16)$$

Note, that for the special case of the elevation angles being zero, the computed distances are identical to that obtained in Ref. [2].

Correspondingly, the vertical component is computed as

$$d_{\min}^V = R_{LOS} \text{ If } |\sigma_{rel} - \sigma_{LOS}| \geq 90^\circ; \text{ ELSE}$$

$$d_{\min}^V = R_{LOS} \sin(\sigma_{rel} - \sigma_{LOS}) \quad (17)$$

For simplicity we will assume a spherical separation requirement around each aircraft, let D_{sep} represent this separation requirement (e.g., a standard separation of 5nm, plus some buffer). A conflict is predicted to occur if $d_{\min} < D_{sep}$ or in other words, the \mathbf{V}_{rel} vector, when projected in time, intersects the sphere of radius D_{sep} around Aircraft B as depicted in Figure 3.

III. Conflict Resolution

For the resolution of this conflict the direction of this relative velocity vector, \mathbf{V}_{rel} must be changed so that its projection line in time does not intersect the sphere but is a tangent to it to avoid conflict. Of course any solution that moves the relative velocity vector outside the cone will work, however the tangential solution will result in an efficient (“*optimal*”) conflict resolution. Also, this change results in the least allowable deviation of all possible deviations to avoid conflict and minimize $\Delta\mathbf{V}$. This can be achieved in many different ways; by changing the direction (heading and/or elevation angle) and/or magnitude (airspeed) of \mathbf{V}_A and/or \mathbf{V}_B , or any combination thereof.

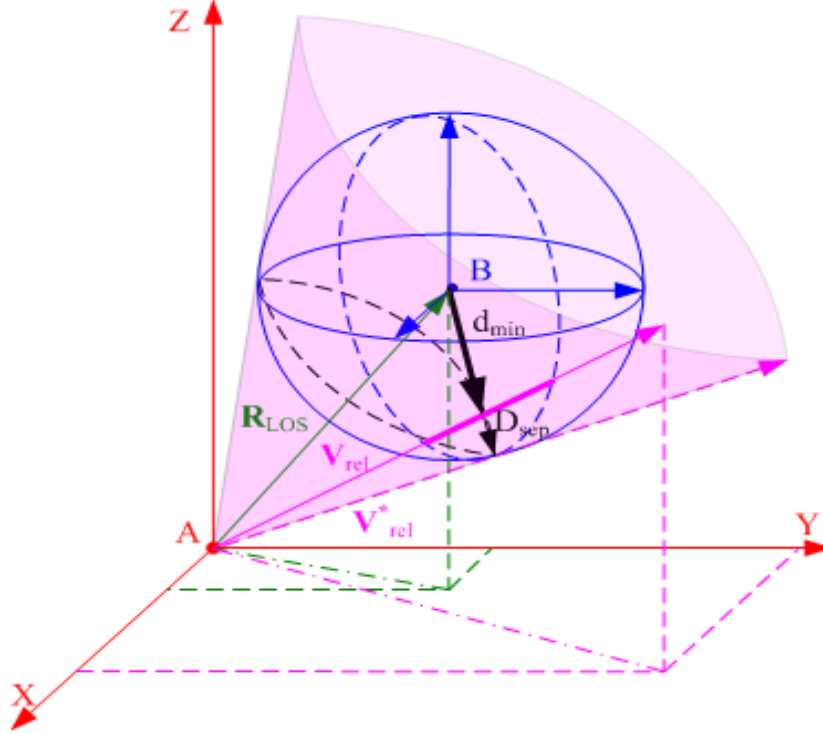


Figure 4: Conflict resolution cone.

Let \mathbf{V}_{rel}^* represent a new relative velocity vector, where χ_{rel}^* and σ_{rel}^* represent the heading and elevation angles respectively, whose projection in time does not intersect the protected zone around Aircraft B. For this new relative vector to be a tangent we have in the horizontal plane, from equation (16)

$$d_{min}^{H*} = R_{LOS} \cos(\sigma_{rel} - \sigma_{LOS}) \sin|\chi_{LOS} - \chi_{rel}^*| = \sqrt{D_{sep}^2 - d_{min}^{V*2}} \quad (18)$$

This equation can then be rearranged to get the new heading angle for the relative velocity vector if we restrict our correction to the horizontal plane only.

$$\begin{aligned} \sin|\chi_{LOS} - \chi_{rel}^*| &= \frac{\sqrt{D_{sep}^2 - d_{min}^{V*2}}}{R_{LOS} \cos(\sigma_{rel} - \sigma_{LOS})} \\ \chi_{rel}^* &= \chi_{LOS} \pm \sin^{-1} \left(\frac{\sqrt{D_{sep}^2 - d_{min}^{V*2}}}{R_{LOS} \cos(\sigma_{rel} - \sigma_{LOS})} \right) \end{aligned} \quad (19)$$

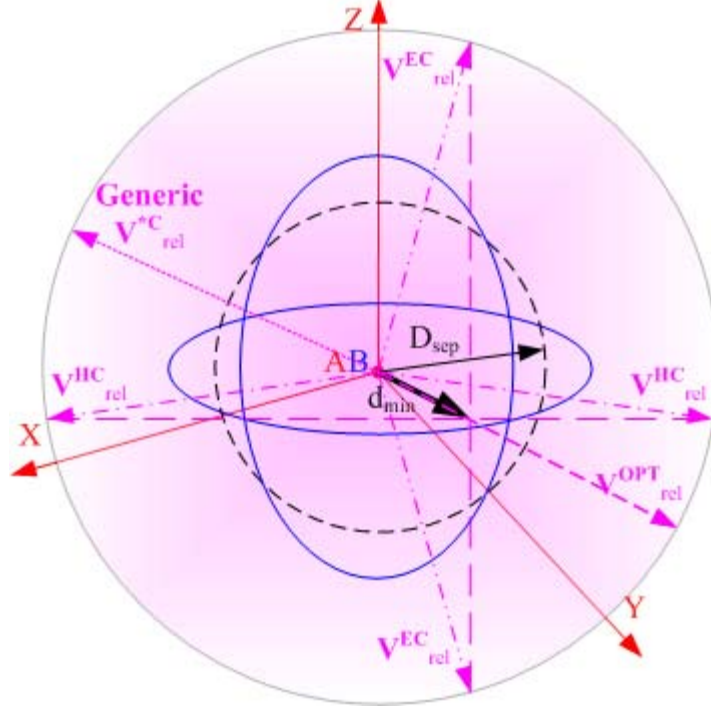


Figure 5: Looking down the conflict resolution cone, resolution options for heading change, elevation change, a generic combination, and an optimal solution are shown.

We will have a total of 4 solutions for χ_{rel}^* , two due to the nature of the inverse sine function (θ and $\pi - \theta$) and each of those will have two solutions due to \pm sign. Only two of these lines will be tangent lines from Aircraft A to the sphere around B while the other two will be 180 degrees off. All four will be in the horizontal plane and all must be tested to see which will achieve the desired separation distance with the minimum deviation.

Similarly we can adjust the relative velocity vector to be tangential in the vertical plane. Going by the same computation as before and using equation (17)

$$d_{min}^{V*} = R_{LOS} \sin|\sigma_{LOS} - \sigma_{rel}^*| = \sqrt{D_{sep}^2 - d_{min}^H{}^2} \quad (20)$$

This will result in a new elevation angle of the relative velocity vector, σ_{rel}^* while keeping the heading angle constant as χ_{rel} .

$$\sigma_{rel}^* = \sigma_{LOS} \pm \sin^{-1} \left(\frac{\sqrt{D_{sep}^2 - d_{min}^H{}^2}}{R_{LOS}} \right) \quad (21)$$

The quantities $\Delta\chi_{rel} = (\chi_{rel}^* - \chi_{rel})$ and $\Delta\sigma_{rel} = (\sigma_{rel}^* - \sigma_{rel})$ are the fundamental parameters, which represents the size of conflict resolution maneuvers in the horizontal and vertical planes. Either or both of the Aircraft may participate in the conflict resolution process and therefore either or both aircraft may contribute to the values of $\Delta\chi_{rel}$ and $\Delta\sigma_{rel}$.

Following the procedure in Ref. [2], let f_A and f_B represents the contribution of Aircraft A and B for $\Delta\chi_{rel}$ where $0 \leq f_{A,B} \leq 1$ and $f_A + f_B = 1$. Similarly g_A and g_B represents the contribution of Aircraft A and B for $\Delta\sigma_{rel}$ where $0 \leq g_{A,B} \leq 1$ and $g_A + g_B = 1$. Although $(f_A + f_B) > 1$ and $(g_A + g_B) > 1$ are possible, the conflict resolution will be inefficient as the corresponding minimum separation distance d_{min} will then exceed separation requirement D_{sep} . Thus for the horizontal plane we have

$$\begin{aligned}\chi_{relA}^* &= \chi_{rel} + f_A(\chi_{rel}^* - \chi_{rel}) \\ \chi_{relB}^* &= \chi_{rel} + f_B(\chi_{rel}^* - \chi_{rel})\end{aligned}\quad (22)$$

Substituting Eq. (19) for χ_{rel}^* into Eq. (22) yields

$$\chi_{relA}^* = \chi_{rel} + f_A \left\{ \chi_{LOS} \pm \sin^{-1} \left(\frac{\sqrt{D_{sep}^2 - d_{min}^{V^2}}}{R_{LOS} \cos(\sigma_{rel} - \sigma_{LOS})} \right) - \chi_{rel} \right\} \quad (23)$$

$$\chi_{relB}^* = \chi_{rel} + f_B \left\{ \chi_{LOS} \pm \sin^{-1} \left(\frac{\sqrt{D_{sep}^2 - d_{min}^{V^2}}}{R_{LOS} \cos(\sigma_{rel} - \sigma_{LOS})} \right) - \chi_{rel} \right\} \quad (24)$$

Similarly for vertical plane

$$\begin{aligned}\sigma_{relA}^* &= \sigma_{rel} + g_A(\sigma_{rel}^* - \sigma_{rel}) \\ \sigma_{relB}^* &= \sigma_{rel} + g_B(\sigma_{rel}^* - \sigma_{rel})\end{aligned}\quad (25)$$

Substituting Eq. (21) for σ_{rel}^* into Eq. (25) yields

$$\sigma_{relA}^* = \sigma_{rel} + g_A \left\{ \sigma_{LOS} \pm \sin^{-1} \left(\frac{\sqrt{D_{sep}^2 - d_{min}^{H^2}}}{R_{LOS}} \right) - \sigma_{rel} \right\} \quad (26)$$

$$\sigma_{relB}^* = \sigma_{rel} + g_B \left\{ \sigma_{LOS} \pm \sin^{-1} \left(\frac{\sqrt{D_{sep}^2 - d_{min}^{H^2}}}{R_{LOS}} \right) - \sigma_{rel} \right\} \quad (27)$$

When $f_A, f_B > 0$ and $f_A + f_B = 1$, $g_A, g_B > 0$ and $g_A + g_B = 1$, it is a cooperative conflict resolution., a non-cooperative conflict resolution corresponds to either of these being 0 or 1. The default values for our situation are $f_A = f_B = g_A = g_B = 0.5$.

From here on we will consider only changes in the heading, elevation or airspeed for conflict resolution maneuvers executed by Aircraft A. The corresponding expressions for Aircraft B can be obtained by substitution of corresponding parameters.

A. Heading Change (HC)

We note that changing the heading angle of Aircraft A to χ_A^* , will result in a new velocity vector \mathbf{V}_A^* with a magnitude V_A^* . From Eq. (13), which relates the heading angle to the X and Y components of the relative velocity vector, we have

$$\left(\frac{\sin \chi_{relA}^*}{\cos \chi_{relA}^*} \right) = \left(\frac{V_B \cos \sigma_B \sin \chi_B - V_A^* \cos \sigma_A \sin \chi_A^*}{V_B \cos \sigma_B \cos \chi_B - V_A^* \cos \sigma_A \cos \chi_A^*} \right) \quad (28)$$

Some algebraic manipulation of Eq. (28) results in the following,

$$\begin{aligned}V_A^* \cos \chi_{relA}^* \cos \sigma_A \sin \chi_A^* - V_A^* \sin \chi_{relA}^* \cos \sigma_A \cos \chi_A^* &= V_B \cos \sigma_B \sin \chi_B \cos \chi_{relA}^* \\ &\quad - V_B \cos \sigma_B \cos \chi_B \sin \chi_{relA}^* \\ \Rightarrow V_A^* \cos \sigma_A \sin(\chi_A^* - \chi_{relA}^*) &= V_B \cos \sigma_B \sin(\chi_B - \chi_{relA}^*)\end{aligned}$$

$$\Rightarrow V_A^* \sin(\chi_A^* - \chi_{relA}^*) = V_B \frac{\cos \sigma_B}{\cos \sigma_A} \sin(\chi_B - \chi_{relA}^*) \quad (29)$$

Here the heading angle of the relative velocity χ_{relA}^* is obtained from Eq. (23).

For a conflict resolution method considering heading change alone (HC), the magnitude of the velocity vector remains constant, $V_A^{HC} = V_A$ and the corresponding heading angle is obtained from Eq. (29)

$$\chi_A^{HC} = \chi_{relA}^* + \sin^{-1} \left\{ \frac{V_B}{V_A} \frac{\cos \sigma_B}{\cos \sigma_A} \sin(\chi_B - \chi_{relA}^*) \right\} \quad (30)$$

Remarks:

- For Eq. (30) to be valid, the argument of \sin^{-1} should not exceed unity. Note that this is trivially satisfied so long as $V_A \cos \sigma_A \geq V_B \cos \sigma_B$. (This result admits solutions for cases when $V_A \leq V_B$, so long as the elevation angles are admissible). For this case, Eq. (30) is valid for both values of χ_{relA}^* obtained from Eq. (23).
- When $V_A \cos \sigma_A < V_B \cos \sigma_B$, the solutions for χ_{relA}^* that are valid here depend on the conflict geometry. Again due to the nature of the inverse sine function we need to consider both solution possibilities (θ and $\pi - \theta$) for χ_A^{HC} . As pointed out in Ref. [2], for cases when one of the solutions for χ_A^{HC} results in a value of χ_{relA}^* that is opposite to the desired direction we discard that solution. In all other cases, both solutions are considered.

Our objective for the conflict resolution is to minimize the change in the magnitude of the velocity vector. The magnitude of the velocity vector change for HC can be obtained as follows

From Eq. (9) we have the original velocity vector of Aircraft A \mathbf{V}_A as

$$\mathbf{V}_A = V_A \cos \sigma_A \cos \chi_A \hat{x} + V_A \cos \sigma_A \sin \chi_A \hat{y} + V_A \sin \sigma_A \hat{z}$$

Due to heading change alone we have the new velocity vector for Aircraft A as \mathbf{V}_A^{HC} , knowing the fact that $V_A^{HC} = V_A$, it is given by

$$\mathbf{V}_A^{HC} = V_A \cos \sigma_A \cos \chi_A^{HC} \hat{x} + V_A \cos \sigma_A \sin \chi_A^{HC} \hat{y} + V_A \sin \sigma_A \hat{z} \quad (31)$$

Therefore by the cosine rule we have

$$\Delta V_A^{HC} = V_A \sqrt{2[1 - \cos(\angle \mathbf{V}_A, \mathbf{V}_A^{HC})]} \quad (32)$$

Where the cosine of the angle between the two vectors is given by, $\cos(\angle \mathbf{V}_A, \mathbf{V}_A^{HC}) = \frac{\mathbf{V}_A \cdot \mathbf{V}_A^{HC}}{V_A^2}$

Substituting for \mathbf{V}_A , \mathbf{V}_A^{HC} and simplifying we get,

$$\cos(\angle \mathbf{V}_A, \mathbf{V}_A^{HC}) = (\cos^2 \sigma_A \cos(\chi_A - \chi_A^{HC}) + \sin^2 \sigma_A).$$

Using this in Eq. (32), we obtain

$$\Delta V_A^{HC} = V_A \cos(\sigma_A) \sqrt{2[1 - \cos(\chi_A - \chi_A^{HC})]} \quad (33)$$

Thus it is clear from Eq. (33) that the desired solution for heading change alone is the one that results in smallest heading change. However, the change also depends on the current elevation of the Aircraft A. Note the result obtained here is very similar to the result obtained in Ref. [2].

B. Elevation Change (EC)

Similarly as with the Heading Change only case, changing the elevation angle of Aircraft A to σ_A^* , results in another new velocity vector \mathbf{V}_A^* with magnitude V_A^* . From Eq. (14) we have

$$\frac{\sin \sigma_{relA}^*}{\cos \sigma_{relA}^*} = \left(\frac{V_{relZ}}{\sqrt{V_{relX}^2 + V_{relY}^2}} \right) \quad (34)$$

Squaring and rearranging Eq. (34) after tedious but simple algebraic manipulation of Eq. (15) leads us

$$V_A^2 (\sin^2 \sigma_A^* \cos^2 \sigma_{relA}^* - \cos^2 \sigma_A^* \sin^2 \sigma_{relA}^*) + V_B^2 (\sin^2 \sigma_B \cos^2 \sigma_{relA}^* - \cos^2 \sigma_B \sin^2 \sigma_{relA}^*) - 2V_A^* V_B (\sin \sigma_A^* \sin \sigma_B \cos^2 \sigma_{relA}^* - \cos \sigma_A^* \cos \sigma_B \sin^2 \sigma_{relA}^* \cos(\chi_A - \chi_B)) = 0$$

Dividing both sides by V_B^2 and simplifying further we get

$$\left(\frac{V_A^*}{V_B} \right)^2 (\sin^2 \sigma_A^* - \sin^2 \sigma_{relA}^*) - 2 \left(\frac{V_A^*}{V_B} \right) (\sin \sigma_A^* \sin \sigma_B \cos^2 \sigma_{relA}^* - \cos \sigma_A^* \cos \sigma_B \sin^2 \sigma_{relA}^* \cos(\chi_A - \chi_B)) = \sin^2 \sigma_{relA}^* - \sin^2 \sigma_B \quad (35)$$

Where, the elevation angle of the relative velocity σ_{relA}^* is obtained from Eq. (26). For a conflict resolution with elevation change alone (EC), we have $V_A^{EC} = V_A$ and the corresponding elevation angle is obtained from Eq. (35). This equation is non-linear and can be solved iteratively.

$$\left(\frac{V_A}{V_B} \right)^2 (\sin^2 \sigma_A^{EC} - \sin^2 \sigma_{relA}^*) - 2 \left(\frac{V_A}{V_B} \right) (\sin \sigma_A^{EC} \sin \sigma_B \cos^2 \sigma_{relA}^* - \cos \sigma_A^{EC} \cos \sigma_B \sin^2 \sigma_{relA}^* \cos(\chi_A - \chi_B)) = \sin^2 \sigma_{relA}^* - \sin^2 \sigma_B \quad (36)$$

Again to be consistent with the objective of the conflict resolution, that is to minimize the change in the magnitude of the velocity vector, due to elevation change alone we have the new velocity vector for Aircraft A as \mathbf{V}_A^{EC} , knowing the fact that $V_A^{EC} = V_A$, it is given by

$$\mathbf{V}_A^{EC} = V_A \cos \sigma_A^{EC} \cos \chi_A \hat{x} + V_A \cos \sigma_A^{EC} \sin \chi_A \hat{y} + V_A \sin \sigma_A^{EC} \hat{z} \quad (37)$$

The cosine of the angle between the \mathbf{V}_A and \mathbf{V}_A^{EC} is given as $\cos(\angle \mathbf{V}_A, \mathbf{V}_A^{EC}) = \frac{\mathbf{V}_A \cdot \mathbf{V}_A^{EC}}{V_A^2}$, Simplifying it

further we get,

$$\cos(\angle \mathbf{V}_A, \mathbf{V}_A^{EC}) = \cos \sigma_A \cos \sigma_A^{EC} \cos^2 \chi_A + \cos \sigma_A \cos \sigma_A^{EC} \sin^2 \chi_A + \sin \sigma_A \sin \sigma_A^{EC} \quad (38)$$

$$= \cos(\sigma_A - \sigma_A^{EC})$$

Therefore the angle between the two vectors is $(\sigma_A - \sigma_A^{EC})$. Then the magnitude of velocity vector change is given as

$$\Delta V_A^{EC} = V_A \sqrt{2[1 - \cos(\sigma_A - \sigma_A^{EC})]} \quad (39)$$

Remarks:

- The expression for ΔV_A^{EC} in Eq. (39) is identical to that obtained for the Heading Change only case in Ref. [2].
- For the special case, when $\chi_A = \chi_B$ or $\chi_A - \chi_B = 2\pi$, Eq. (36) can be re-arranged to obtain,

$$\frac{V_A \sin(\sigma_A^* - \sigma_{relA}^*)}{V_B \sin(\sigma_B + \sigma_{relA}^*)} = \frac{V_A \sin(\sigma_A^* - \sigma_{relA}^*) - V_B \sin(\sigma_B - \sigma_{relA}^*)}{V_A \sin(\sigma_A^* + \sigma_{relA}^*) - V_B \sin(\sigma_B + \sigma_{relA}^*)}$$

The above provides a ratio of the components of the respective aircraft velocities, perpendicular to the σ_{relA}^* direction.

C. Speed Change (SC)

For a conflict resolution with a speed change alone (SC), we first consider the horizontal plane where we found values for χ_{relA}^* . Recall that these angles are aircraft A's portion of the modified relative velocity vector where we restricted the modification to the horizontal plane. We now want to derive the new velocity vector for aircraft 'A' that will give the relative velocity vector the desired heading χ_{relA}^* . In this case the aircrafts heading and elevation angles remain constant and only the magnitude of the vector is changed. The new airspeed can be obtained from Eq. (29) as

$$V_A^{SC} = V_B \frac{\cos \sigma_B \sin(\chi_B - \chi_{relA}^*)}{\cos \sigma_A \sin(\chi_A - \chi_{relA}^*)} \quad (40)$$

Alternately, doing the same as before in the vertical plane where we found σ_{relA}^* , keeping heading and elevation angles are constant, the corresponding airspeed can be obtained from Eq. (35) as

$$\begin{aligned} \left(\frac{V_A^{SC}}{V_B} \right)^2 \left(\sin^2 \sigma_A - \sin^2 \sigma_{relA}^* \right) - 2 \left(\frac{V_A^{SC}}{V_B} \right) \left(\sin \sigma_A \sin \sigma_B \cos^2 \sigma_{relA}^* - \cos \sigma_A \cos \sigma_B \sin^2 \sigma_{relA}^* \cos(\chi_A - \chi_B) \right) \\ = \sin^2 \sigma_{relA}^* - \sin^2 \sigma_B \end{aligned} \quad (41)$$

Four solutions for V_A^{SC} are obtained, two for the horizontal plane and two for the vertical plane, each set corresponding to the two values of χ_{relA}^* and σ_{relA}^* provided by Eq. (23) and Eq. (26).

The magnitude of the velocity vector change for speed change alone is given by

$$\Delta V_A^{SC} = |V_A^{SC} - V_A| \quad (42)$$

Our objective is to minimize this change in the magnitude of velocity vector, thus the desired solution for V_A^{SC} is the one which results in a smaller speed change. Another factor that must be taken into account while doing a conflict resolution with speed change alone is that the resulting value of V_A^{SC} must lie between the airspeed bounds imposed by aircraft performance. If all the four speeds are not valid, then the conflict cannot be resolved by speed change alone.

Remarks:

- Note that Eq. (40) and Eq. (41) provide two possible mechanisms to obtain a speed change. An important observation can be made in Eq. (40) that is evident only when the 3-D engagement is considered. For large elevations close to 90 degrees, the speed change obtained from Eq. (40) is prone to errors (cosines of the angles tend to zero). While this seems to be a naive observation for the two aircraft engagement, as near 90 degree elevations would be seem to avoid conflict, this is not the case with multiple aircraft engagement, especially when vertically spaced aircrafts need to be maneuvered during “climb” and “descent” phases.
- For cases when the elevation angles are small, Eq. (40) is used for calculating the speed change, while Eq. (41) is used when the elevation angles are large.

D. Heading-Speed Change (HSC)

Let χ_A^{HSC} and V_A^{HSC} denote the heading change and speed change respectively. In this case the elevation angle will remain constant σ_A .

Eq. (29) is modified according to the heading-speed combination change and is re-written as

$$V_A^{HSC} \sin(\chi_{relA}^* - \chi_A^{HSC}) = V_B \frac{\cos \sigma_B}{\cos \sigma_A} \sin(\chi_{relA}^* - \chi_B) \quad (43)$$

In order to solve this equation we will need one more relationship between the speed and heading angle of the desired relative velocity. If we examine the situation more closely, it can be seen in Figure 6 that the optimal heading-speed change combination will result when a line connecting the head of the vector V_A and the head of the

vector \mathbf{V}_A^{HSC} is perpendicular to the new relative velocity vector \mathbf{V}_{relA}^* which is at a tangent to the protected sphere formed around aircraft 'B'.

$$V_A^{HSC} \cos(\chi_{relA}^* - \chi_A^{HSC}) \cos(\sigma_{relA} - \sigma_A) = V_A \cos(\chi_{relA}^* - \chi_A) \cos(\sigma_{relA} - \sigma_A) \quad (44)$$

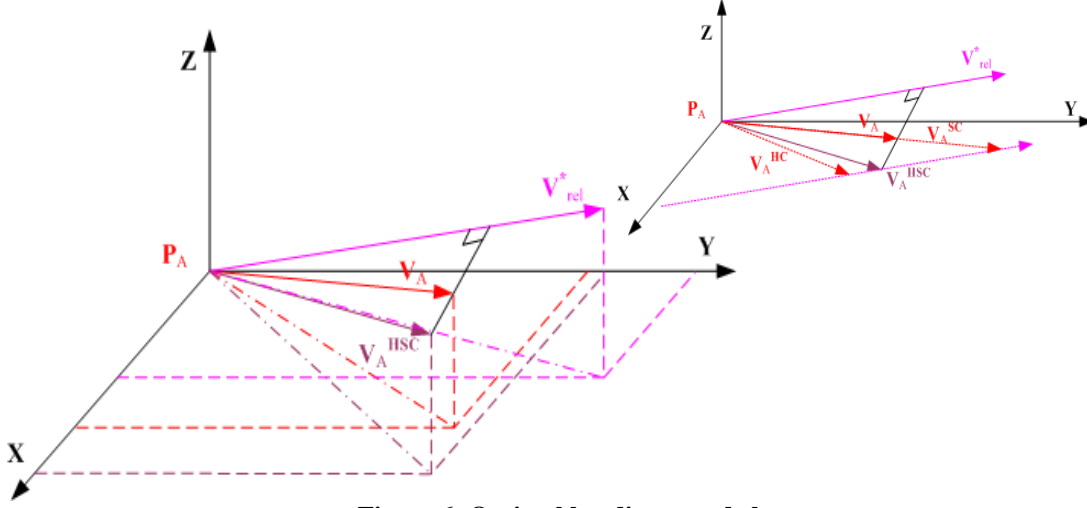


Figure 6: Optimal heading-speed change vector.

Now, dividing equation (43) by (44) gives

$$\tan(\chi_{relA}^* - \chi_A^{HSC}) = \frac{V_B \cos \sigma_B \sin(\chi_{relA}^* - \chi_B)}{V_A \cos \sigma_A \cos(\chi_{relA}^* - \chi_A)}$$

and solving for the heading change, χ_A^{HSC} , we obtain

$$\chi_A^{HSC} = \chi_{relA}^* - \tan^{-1} \left[\frac{V_B \cos \sigma_B \sin(\chi_{relA}^* - \chi_B)}{V_A \cos \sigma_A \cos(\chi_{relA}^* - \chi_A)} \right] \quad (45)$$

Thus Eq. (44) and Eq. (45) are solved simultaneously to obtain the solution for the optimal heading and speed change assuming elevation is kept constant.

As before, the magnitude for the change in velocity vector for the optimal heading-speed change is obtained from cosine rule. $\Delta V_A^{HSC} = \sqrt{(V_A^{HSC})^2 + V_A^2 - 2V_A^{HSC}V_A \cos(\angle \mathbf{V}_A^{HSC}, \mathbf{V}_A)}$

Where the cosine of the angle between the two vectors is given as $\cos(\angle \mathbf{V}_A^{HSC}, \mathbf{V}_A) = \frac{\mathbf{V}_A^{HSC} \cdot \mathbf{V}_A}{V_A^{HSC} V_A}$

E. Elevation-Speed Change (ESC)

Let σ_A^{ESC} and V_A^{ESC} denote the elevation change and speed change respectively. In this case the heading angle of aircraft 'A' is maintained constant χ_A .

Following along the same lines as before, Eq. (35) is modified according to the elevation-speed combination change and is written as

$$\begin{aligned} & \left(\frac{V_A^{ESC}}{V_B} \right)^2 (\sin^2 \sigma_A^{ESC} - \sin^2 \sigma_{relA}^*) - 2 \left(\frac{V_A^{ESC}}{V_B} \right) \left(\sin \sigma_A^{ESC} \sin \sigma_B \cos^2 \sigma_{relA}^* - \right. \\ & \left. \cos \sigma_A^{ESC} \cos \sigma_B \sin^2 \sigma_{relA}^* \cos(\chi_A^{ESC} - \chi_B) \right) \\ & = \sin^2 \sigma_{relA}^* - \sin^2 \sigma_B \end{aligned} \quad (46)$$

With the same justification used in the heading-speed combination we can use the following relationship between the speed and elevation angle of the desired relative velocity. The optimal elevation-speed change combination will

result when a line connecting the head of the vector \mathbf{V}_A and the head of the vector \mathbf{V}_A^{ESC} is perpendicular to the new relative velocity vector \mathbf{V}_{relA}^* which is tangent to the protected sphere formed around aircraft 'B'.

$$V_A^{ESC} \cos(\chi_{relA} - \chi_A) \cos(\sigma_{relA}^* - \sigma_A^{ESC}) = V_A \cos(\chi_{relA} - \chi_A) \cos(\sigma_{relA}^* - \sigma_A) \quad (47)$$

Eq. (46) and Eq. (47) are solved iteratively to give the solution for the optimal elevation and speed change assuming heading is kept constant.

For this resolution strategy, the magnitude for the change in velocity vector for the optimal elevation-speed change is obtained from cosine rule.

$$\Delta V_A^{ESC} = \sqrt{(V_A^{ESC})^2 + V_A^2 - 2V_A^{ESC}V_A \cos(\angle \mathbf{V}_A^{ESC}, \mathbf{V}_A)}$$

Where the cosine of the angle between the two vectors is given as $\cos(\angle \mathbf{V}_A^{ESC}, \mathbf{V}_A) = \frac{\mathbf{V}_A^{ESC} \cdot \mathbf{V}_A}{V_A^{ESC} V_A}$

F. Heading-Elevation Change (HEC)

Let χ_A^{HEC} and σ_A^{HEC} denote the heading change and elevation change respectively. In this case the magnitude if the velocity vector will remain constant such that, i.e. $V_A^{HEC} = V_A$

Eq. (29) and Eq. (35) are now modified according to the heading-elevation combination change and written as

$$V_A \sin(\chi_{relA}^* - \chi_A^{HEC}) = V_B \frac{\cos \sigma_B}{\cos \sigma_A^{HEC}} \sin(\chi_{relA}^* - \chi_B) \quad (48)$$

$$\begin{aligned} \left(\frac{V_A}{V_B}\right)^2 \left(\sin^2 \sigma_A^{HEC} - \sin^2 \sigma_{relA}^*\right) - 2 \left(\frac{V_A}{V_B}\right) \left(\frac{\sin \sigma_A^{HEC} \sin \sigma_B \cos^2 \sigma_{relA}^*}{\cos \sigma_A^{HEC} \cos \sigma_B \sin^2 \sigma_{relA}^*} \cos(\chi_A^{HEC} - \chi_B) \right) \\ = \sin^2 \sigma_{relA}^* - \sin^2 \sigma_B \end{aligned} \quad (49)$$

Equations (48) and (49) can then be solved simultaneously to get the new heading and elevation angles. As before, the magnitude for the change in velocity vector for the optimal heading-elevation change is obtained from the cosine rule.

$$\Delta V_A^{HEC} = \sqrt{(V_A^{HEC})^2 + V_A^2 - 2V_A^{HEC}V_A \cos(\angle \mathbf{V}_A^{HEC}, \mathbf{V}_A)}$$

Where the cosine of the angle between the two vectors is given as $\cos(\angle \mathbf{V}_A^{HEC}, \mathbf{V}_A) = \frac{\mathbf{V}_A^{HEC} \cdot \mathbf{V}_A}{V_A^{HEC} V_A}$

Remarks:

- This strategy seeks to combine Eq. (48) and Eq. (49) and find a solution for σ_A^{HEC} and χ_A^{HEC} subject to minimizing, ΔV_A^{HEC} . The sub-problem for optimization is posed as, $\text{Min}_{\sigma_A^{HEC}, \chi_A^{HEC}} \Delta V_A^{HEC}$, subject to Eq. (48) and Eq. (49).

G. Optimal (Heading-Elevation-Speed Combination) Change (OPT)

Let χ_A^{OPT} , σ_A^{OPT} and V_A^{OPT} denote the optimal heading, elevation and airspeed respectively. From Fig. 6 we observe that the line connecting the head of vectors \mathbf{V}_A and \mathbf{V}_A^{OPT} is perpendicular to the new relative velocity vector \mathbf{V}_{relA}^* which is tangent to the protected sphere formed around Aircraft 'B'. From this geometric consideration we have

$$V_A^{OPT} \cos(\chi_{relA}^* - \chi_A^{OPT}) \cos(\sigma_{relA}^* - \sigma_A^{OPT}) = V_A \cos(\chi_{relA}^* - \chi_A) \cos(\sigma_{relA}^* - \sigma_A) \quad (50)$$

Eq. (29) and Eq. (35) are changed according to optimal heading-elevation-speed combination and written as

$$V_A^{OPT} \sin(\chi_A^{OPT} - \chi_{relA}^*) = V_B \frac{\cos \sigma_B}{\cos \sigma_A^{OPT}} \sin(\chi_B - \chi_{relA}^*) \quad (51)$$

$$\begin{aligned} & \left(\frac{V_A^{OPT}}{V_B} \right)^2 \left(\sin^2 \sigma_A^{OPT} - \sin^2 \sigma_{relA}^* \right) - 2 \left(\frac{V_A^{OPT}}{V_B} \right) \left(\frac{\sin \sigma_A^{OPT} \sin \sigma_B \cos^2 \sigma_{relA}^* - \cos \sigma_A^{OPT} \cos \sigma_B \sin^2 \sigma_{relA}^* \cos(\chi_A^{OPT} - \chi_B)}{\cos \sigma_A^{OPT} \cos \sigma_B \sin^2 \sigma_{relA}^* \cos(\chi_A^{OPT} - \chi_B)} \right) \\ & = \sin^2 \sigma_{relA}^* - \sin^2 \sigma_B \end{aligned} \quad (52)$$

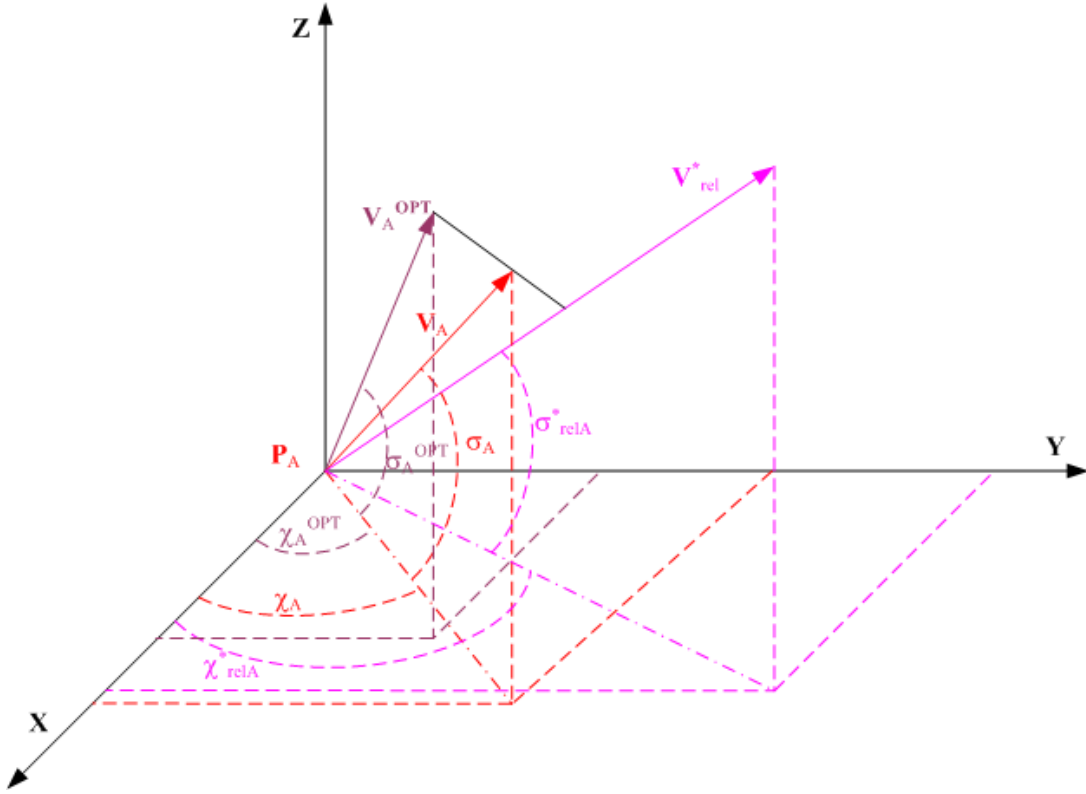


Figure 7: Solution for Heading-Elevation-Speed Combination

Dividing Eq. (50) by Eq. (51) yields

$$\tan(\chi_{relA}^* - \chi_A^{OPT}) = \frac{V_B}{V_A} \frac{\cos \sigma_B}{\cos \sigma_A^{OPT}} \frac{\sin(\chi_{relA}^* - \chi_B) \cos(\sigma_{relA}^* - \sigma_A^{OPT})}{\cos(\chi_{relA}^* - \chi_A) \cos(\sigma_{relA}^* - \sigma_A)} \quad (53)$$

The optimal heading angle can be obtained from Eq. (53) above as

$$\chi_A^{OPT} = \chi_{relA}^* - \tan^{-1} \left\{ \frac{V_B}{V_A} \frac{\cos \sigma_B}{\cos \sigma_A^{OPT}} \frac{\sin(\chi_{relA}^* - \chi_B) \cos(\sigma_{relA}^* - \sigma_A^{OPT})}{\cos(\chi_{relA}^* - \chi_A) \cos(\sigma_{relA}^* - \sigma_A)} \right\} \quad (54)$$

As before, Eq. (50), Eq. (51) and Eq. (52) need to be solved simultaneously to find the values of optimal heading angle, optimal elevation angle and optimal airspeed.

There will be two sets of solutions for $(\chi_A^{OPT}, \sigma_A^{OPT}, V_A^{OPT})$, resulting from two values of χ_{relA}^* and σ_{relA}^* obtained from Eq. (23) and Eq. (26). The solution to this combination is posed as an optimization sub-problem, i.e., $\text{Min}_{\sigma_A^{OPT}, \chi_A^{OPT}, V_A^{OPT}} \Delta V_A^{OPT}$, subject to Eq. (50), (51) and (52).

ΔV_A^{OPT} is computed using,

$$\Delta V_A^{OPT} = \sqrt{(V_A^{OPT})^2 + V_A^2 - 2V_A^{OPT}V_A \cos(\angle \mathbf{V}_A^{OPT}, \mathbf{V}_A)} \quad (55)$$

and the cosine of the angle between the two vectors is given as $\cos(\angle \mathbf{V}_A^{OPT}, \mathbf{V}_A) = \frac{\mathbf{V}_A^{OPT} \cdot \mathbf{V}_A}{V_A^{OPT} V_A}$

Note that the optimal velocity vector is then given as,

$$\mathbf{V}_A^{OPT} = V_A^{OPT} \cos \sigma_A^{OPT} \cos \chi_A^{OPT} \hat{x} + V_A^{OPT} \cos \sigma_A^{OPT} \sin \chi_A^{OPT} \hat{y} + V_A^{OPT} \sin \sigma_A^{OPT} \hat{z} \quad (56)$$

For this case, the cosine of angle between these two vectors after some simple algebraic manipulation is obtained as

$$\cos(\angle \mathbf{V}_A^{OPT}, \mathbf{V}_A) = \cos \sigma_A^{OPT} \cos \chi_A^{OPT} \cos \sigma_A [\cos \chi_A + \sin \chi_A] + \sin \sigma_A \sin \sigma_A^{OPT} \quad (57)$$

Note, that the value of V_A^{OPT} calculated is valid only if it lies between the airspeed bounds imposed by the aircraft performance. If the value of V_A^{OPT} violates an airspeed bound, the modified values of V_A^{OPT} is given by

$$\begin{aligned} (V_A^{OPT})_{\text{mod}} &= V_{\min} \quad \text{if } V_A^{OPT} < V_{\min} \\ (V_A^{OPT})_{\text{mod}} &= V_{\max} \quad \text{if } V_A^{OPT} > V_{\max} \end{aligned}$$

For such cases, the heading and elevation angles are adjusted to compensate for the limiting the speed. This is done by replacing V_A with the modified value of V_A^{OPT} in Eq. (29) and Eq. (35) and computing the modified values of heading and elevation angles. Also while computing the magnitude for the change in velocity vector by Eq. (50); we replace the values with their modified values.

IV. Simulation

The simulation of the above-mentioned conflict detection and resolution strategies are summarized in Figure 8. The implementations were carried out in MATLAB 6.5 and the optimization sub-problems were setup in the FSOLVE framework in the Optimization Toolbox.

The intent of this design is to run the conflict avoidance algorithm only once for each conflict. And if for some reason the minimum path deviation solution does not resolve the conflict then we precede to the second least path deviation and so on. In some cases there are multiple solutions of the same deviation amount where only one combination will give a valid resolution. In these cases the second and third least path deviation may only be numbered such because they follow later in the list, where the actual path deviations are equal to the first.

V. Results

The simulation has only been run for a few preliminary test cases to check the validity of the methodology. The first case is a head on situation where Aircrafts A and B are some distance apart traveling directly towards each other at the same speed. For an example, in Figure 9 Aircraft A starts at the origin (0, 0, 0) and has a destination of (20, 20, 0), and aircraft B starts at (20, 20, 0) and has a destination of (0, 0, 0), if we consider the units to be nautical miles, that would put the two aircraft 28.3 nm apart. If the two aircraft have speeds of 180 knts or 3 nm/min, we can see that the conflict avoidance maneuver will take approximately 90 minutes and that the minimum approach will occur at the half way point. Figure 10 shows the Elevation change solution for the same situation. In both figures the straight line on the conflict avoidance plot represents the desired flight paths and the sphere represents a 5 nm protected zone at the point of conflict.

There is no speed change solution for this case and the heading-speed combination gives the same results as the heading change alone which we would expect since there is no speed solution. The elevation-speed combination should give the same results but we found a few difficulties in getting a good solution using the FSOLVE routine in MATLAB. For future test we hope to implement a more robust solver for the complex cases.

The second case we ran was a 90 degree intersection again with the two aircraft having the same speed. Here Aircraft A again starts at the origin (0, 0, 0) and is destined for (20, 20, 0), and aircraft B starts at (0, 20, 0) and is destined for (20, 0, 0). The velocities are the same as for the previous case, 3nm/min.

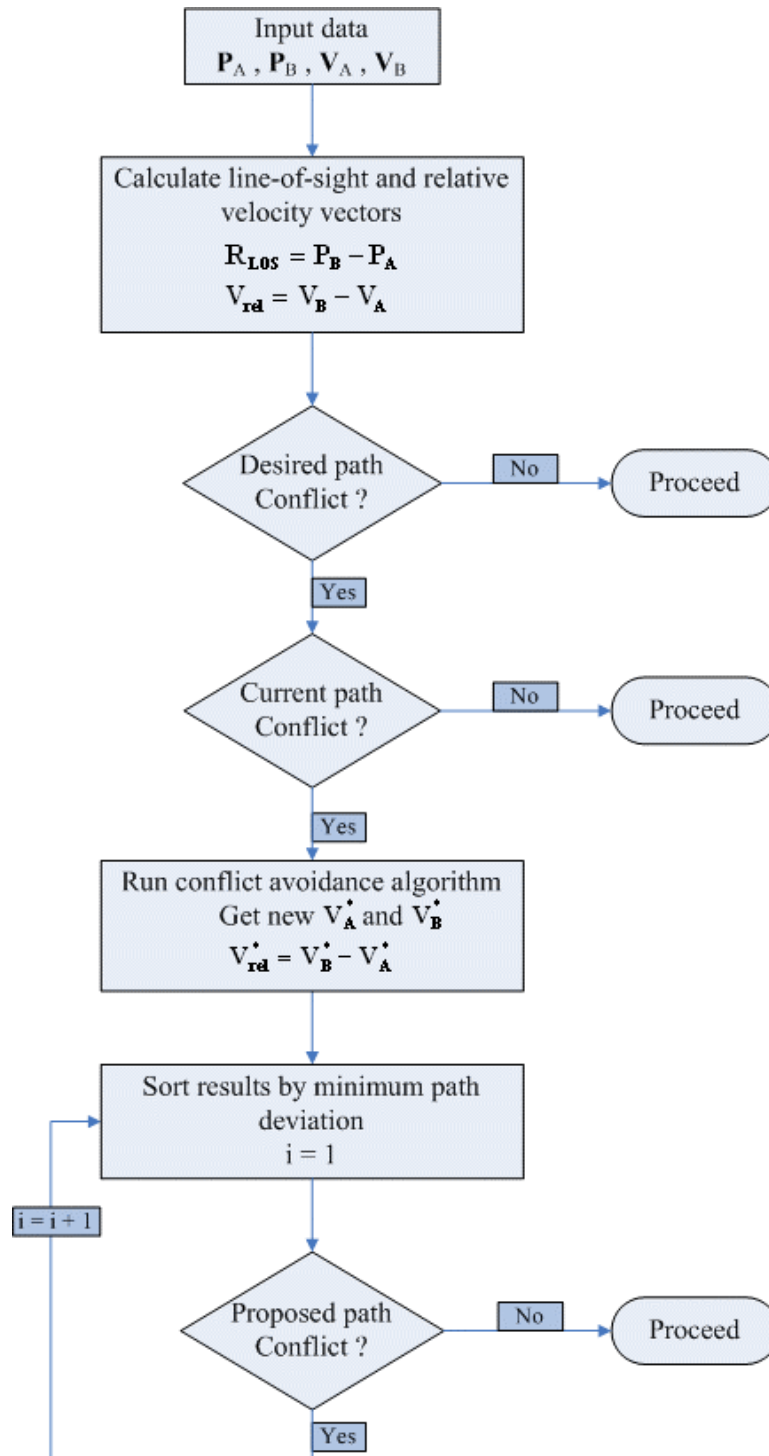


Figure 8: Simulation flow chart.

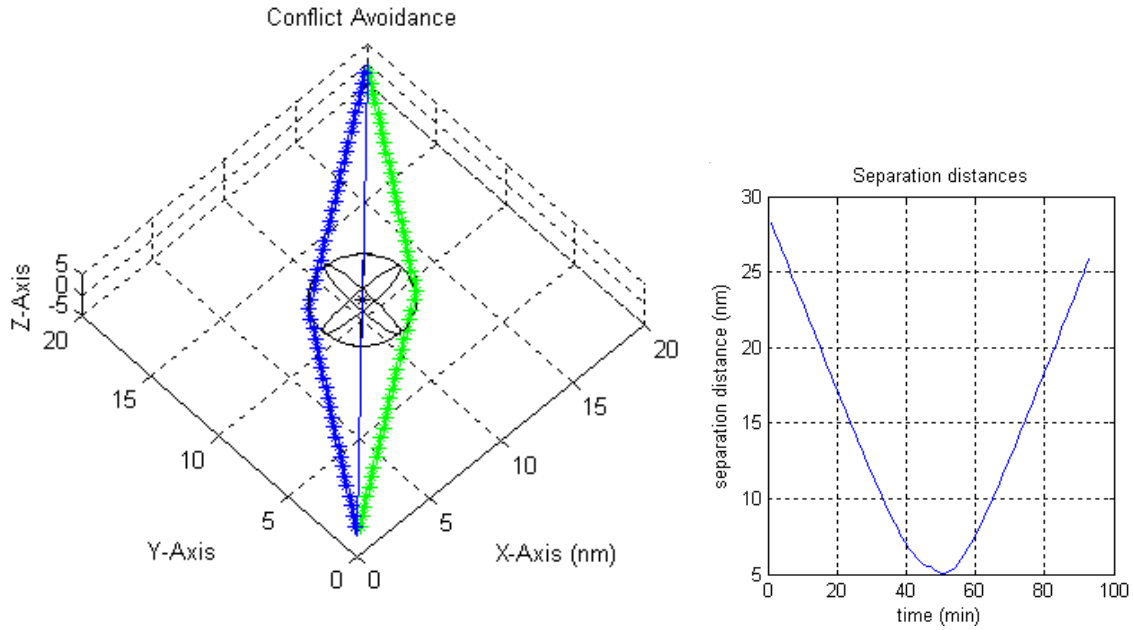


Figure 9: Heading Change resolution for head on conflict.

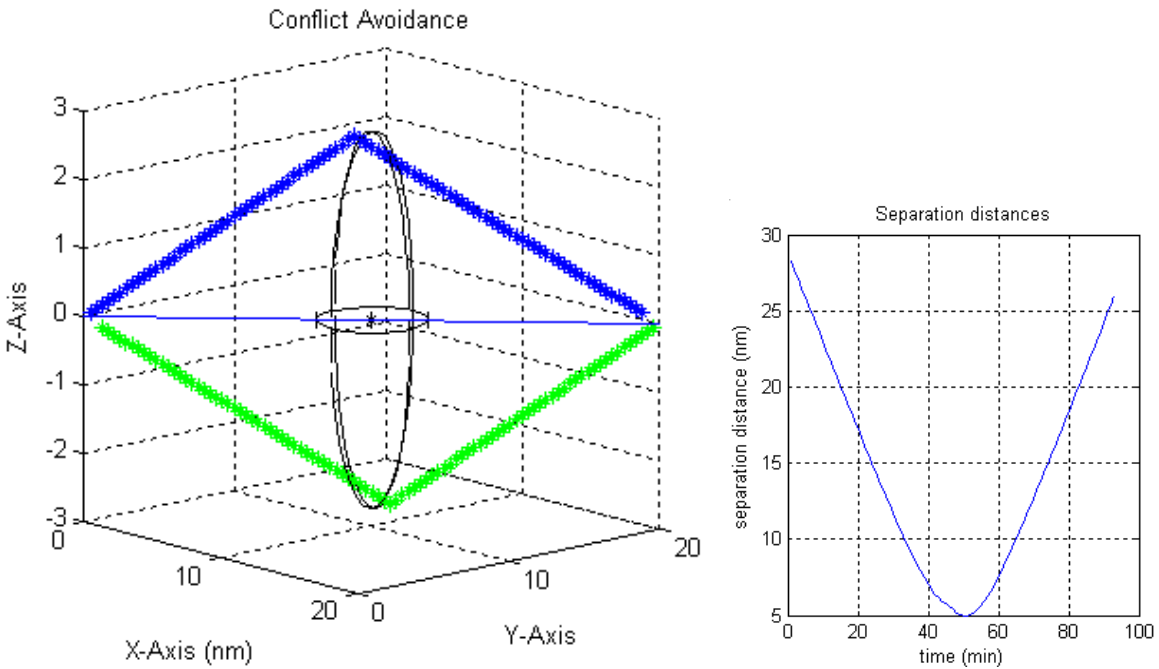


Figure 10: Elevation Change resolution for head on conflict.

Fig. 13 shows the speed change solution for this case. In this figure the speed change can be recognized by the position markers for each time step. Notice that for aircraft B the speed is much faster for the first part of its path and also for aircraft A the speed is much slower for the first part of its path and then the speeds then equal out once the conflict is resolved.

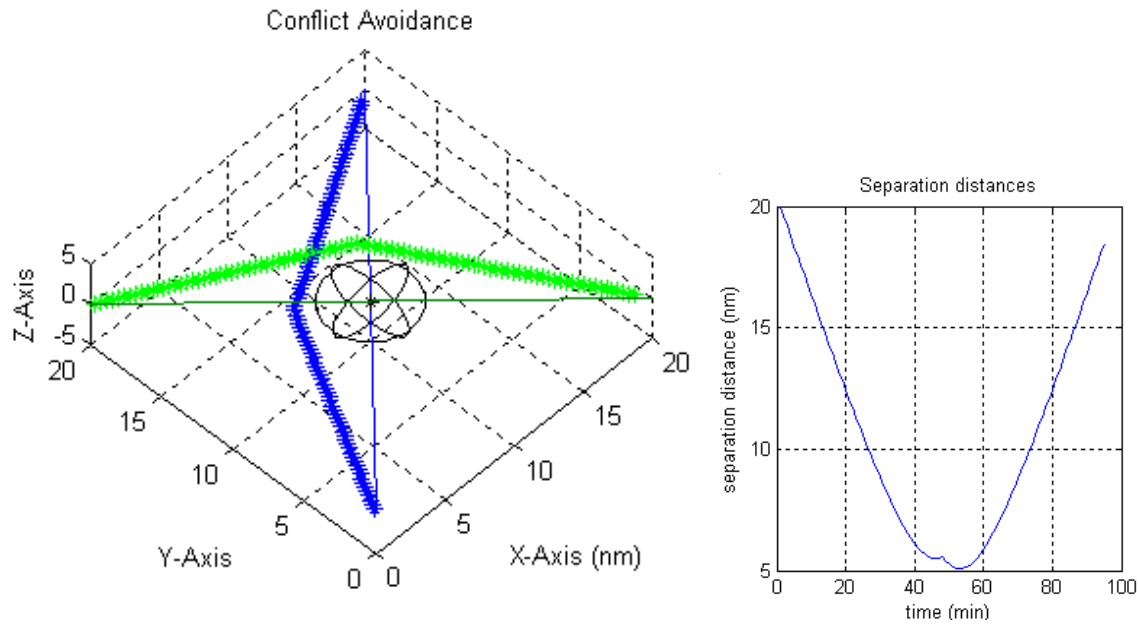


Figure 11: Heading Change resolution for 90deg intersection.

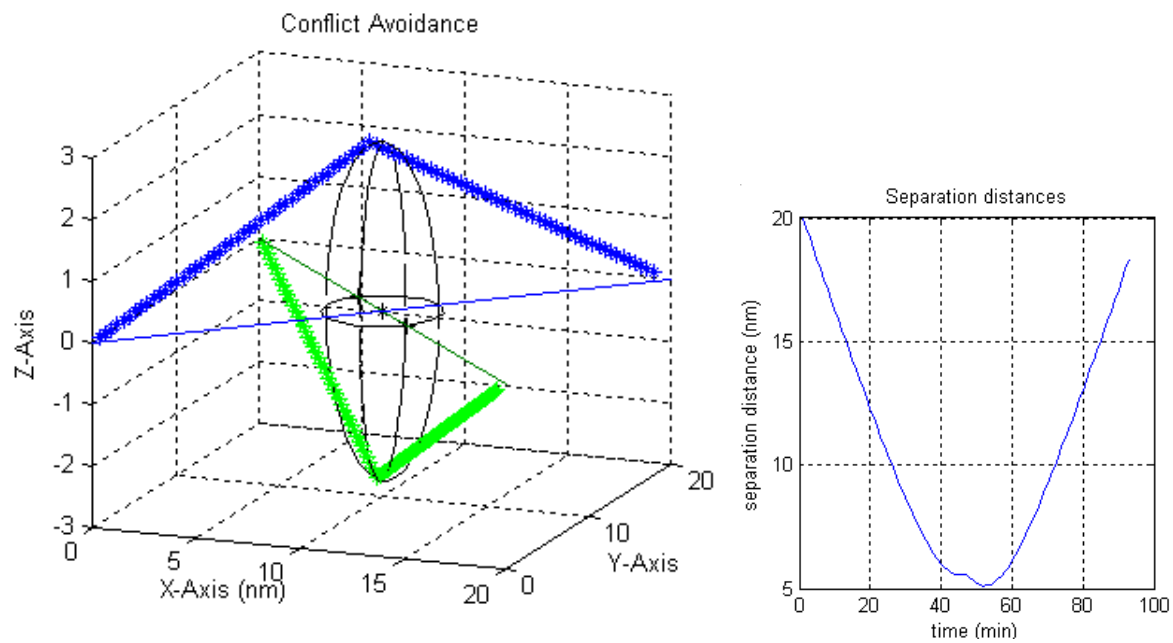


Figure 12: Elevation Change resolution for 90deg intersection.

For the final resolution decision, the results from all of the various combinations are compared and the overall minimum path deviation is chosen. The ideal result combination varies depending on the conflict geometry and each combination has a time when it will be optimum.

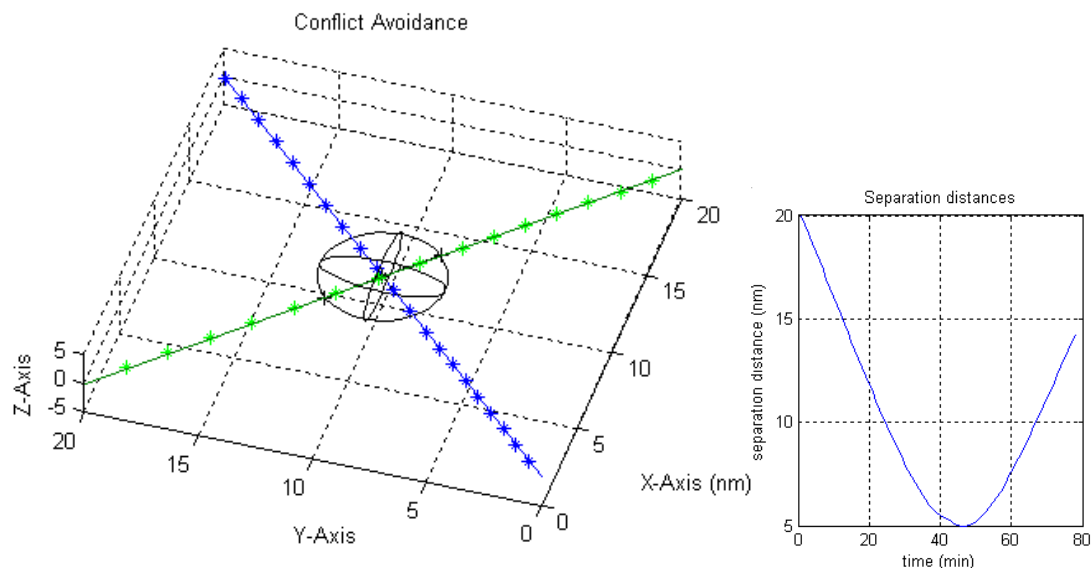


Figure 13: Speed Change resolution for 90deg intersection.

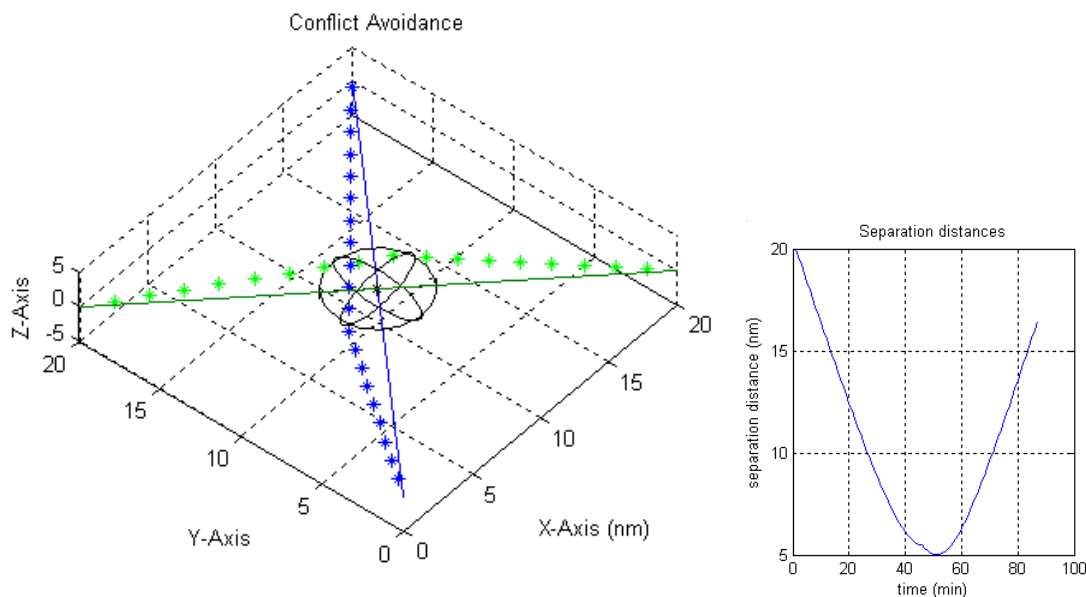


Figure 14: Heading and Speed Change resolution for 90deg intersection.

VI. Summary and Conclusions

This paper considered the problem of avoidance of conflict or collision between two aircraft in a 3-D environment utilizing current positions and velocities using a mixed geometric and collision cone approach. Analytical results were obtained for certain special cases and numerical optimization techniques were employed to search for solutions to the most general cases. This method provided very nice results for the paired down 2-dimensional restrictions in the horizontal and vertical planes. However due to the nature of the problem setup involving several transcendental equations, the nonlinear equation solver has a tendency to get stuck at spurious updates in more complex scenarios. At this point, several alternative approaches (including developing a more robust solver) to obtain the solutions are being researched.

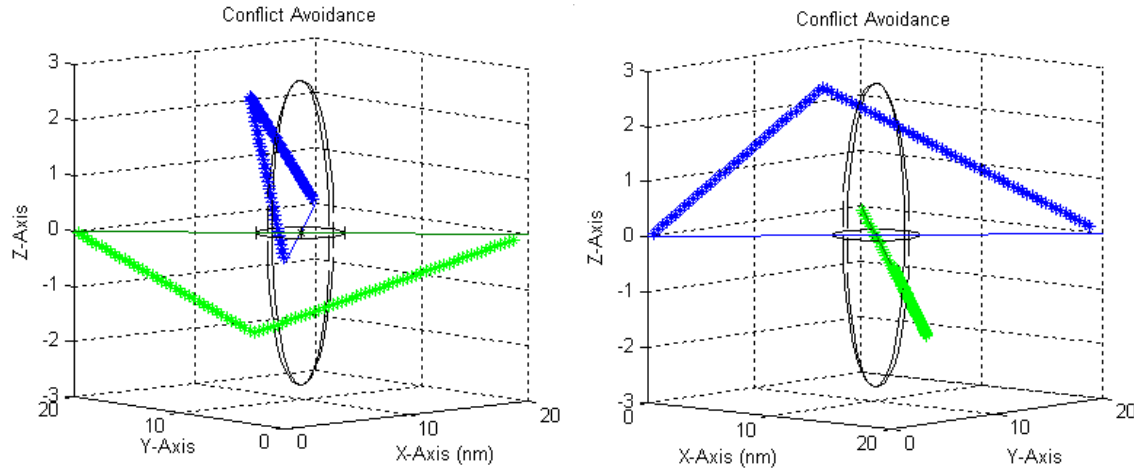


Figure 15: Heading and Elevation Change Resolution to 90deg intersection.

References

- ¹Kuchar, J., and Yang, L., "Survey of Conflict Detection and Resolution Modeling Methods", *Proceedings of the AIAA Guidance, Navigation and Control Conference*, August 1997, pp 1388-1397.
- ²Billimoria Karl D., "A geometric Optimization Approach to Aircraft Conflict Resolution", *Proceedings of the AIAA Guidance, Navigation and Control Conference*, Paper No., AIAA 2000-4265, August 2000, Denver, Colorado
- ³A. Chakravarthy and D. Ghose, "Obstacle Avoidance in a Dynamic Environment: A Collision Cone Approach", *IEEE Transactions on Systems, Man and Cybernetics*, Vol. 28, No. 5, , pp 562-574, September 1998.
- ⁴K. Fujimura, "*Motion Planning in Dynamic Environments*", Tokyo, Japan: Springer-Verlag, 1991
- ⁵Y. K. Hwang and N. Ahuja, "Gross motion planning—A survey", *ACM Computer Survey*, vol. 24, pp. 219–291, Sept. 1992
- ⁶J. T. Schwartz and M. Sharir, "A survey of motion planning and related geometric algorithms", *Artificial Intelligence*, vol. 37, no. 1–3, pp. 157–169, Dec. 1988.
- ⁷J. T. Schwartz and C. K. Yap, Eds., "*Advances in Robotics Vol. I: Algorithmic and Geometric Aspects of Robotics*", Hillsdale, NJ: Lawrence Erlbaum, 1987.
- ⁸J. C. Latombe, "*Robot Motion Planning*", Boston, MA: Kluwer, 1991.